



Public Health  
England



# **NHS Breast Screening Programme Equipment Report**

Technical evaluation of GE Healthcare  
Senographe Pristina digital breast  
tomosynthesis system

## About Public Health England

Public Health England exists to protect and improve the nation's health and wellbeing, and reduce health inequalities. We do this through world-leading science, knowledge and intelligence, advocacy, partnerships and the delivery of specialist public health services. We are an executive agency of the Department of Health and Social Care, and a distinct delivery organisation with operational autonomy. We provide government, local government, the NHS, Parliament, industry and the public with evidence-based professional, scientific and delivery expertise and support.

Public Health England, Wellington House, 133-155 Waterloo Road, London SE1 8UG

Tel: 020 7654 8000 [www.gov.uk/phe](http://www.gov.uk/phe)

Twitter: [@PHE\\_uk](https://twitter.com/PHE_uk) Facebook: [www.facebook.com/PublicHealthEngland](https://www.facebook.com/PublicHealthEngland)

## About PHE Screening

Screening identifies apparently healthy people who may be at increased risk of a disease or condition, enabling earlier treatment or informed decisions. National population screening programmes are implemented in the NHS on the advice of the UK National Screening Committee (UK NSC), which makes independent, evidence-based recommendations to ministers in the 4 UK countries. PHE advises the government and the NHS so England has safe, high quality screening programmes that reflect the best available evidence and the UK NSC recommendations. PHE also develops standards and provides specific services that help the local NHS implement and run screening services consistently across the country.

PHE Screening, Floor 2 Zone B, Skipton House, 80 London Road, London SE1 6LH

[www.gov.uk/phe/screening](http://www.gov.uk/phe/screening) Twitter: [@PHE\\_Screening](https://twitter.com/PHE_Screening) Blog: [phescreening.blog.gov.uk](http://phescreening.blog.gov.uk)

For queries relating to this document, please contact: [phe.screeninghelpdesk@nhs.net](mailto:phe.screeninghelpdesk@nhs.net)

© Crown copyright 2018

You may re-use this information (excluding logos) free of charge in any format or medium, under the terms of the Open Government Licence v3.0. To view this licence, visit [OGL](https://www.ogcl.gov.uk). Where we have identified any third party copyright information you will need to obtain permission from the copyright holders concerned.

Published January 2019

PHE publications

gateway number: 2018754

PHE supports the UN

Sustainable Development Goals



# Contents

About Public Health England	2
About PHE Screening	2
Contents	3
Executive summary	4
1. Introduction	5
1.1 Testing procedures and performance standards for digital mammography	5
1.2 Objectives	5
2. Methods	6
2.1 System tested	6
2.2 Dose and contrast-to-noise ratio using AEC	8
2.3 Image quality measurements	10
2.4 Geometric distortion and reconstruction artefacts	10
2.5 Alignment	11
2.6 Image uniformity and repeatability	12
2.7 Detector response	12
2.8 Timings	12
2.9 Modulation transfer function	13
2.10 Local dense area	13
3. Results	15
3.1 Dose and contrast-to-noise ratio using AEC	15
3.2 Image quality measurements	17
3.3 Geometric distortion and resolution between focal planes	19
3.4 Alignment	21
3.5 Image uniformity and repeatability	21
3.6 Detector response	22
3.7 Timings	22
3.8 Modulation Transfer Function	22
3.9 Local dense area	24
4. Discussion	26
5. Conclusions	28
References	29

## Executive summary

The technical performance of the GE Senographe Pristina digital breast tomosynthesis system was tested in tomosynthesis mode. The evaluation of the performance in 2D mode is published as a separate report. The mean glandular dose (MGD) to the standard breast was found to be 1.23mGy, which is below the dose limiting value of 2.5mGy for tomosynthesis in the EUREF protocol.

Technical performance of this equipment was found to be satisfactory, so that the system could proceed to practical evaluation in a screening centre. This report provides baseline measurements of the equipment performance including:

- dose
- contrast detail detection
- contrast-to-noise ratio (CNR)
- reconstruction artefacts, z-resolution
- detector response
- projection modulation transfer function (MTF)

# 1. Introduction

## 1.1 Testing procedures and performance standards for digital mammography

This report is one of a series evaluating commercially available digital breast tomosynthesis systems on behalf of the NHS Breast Screening Programme (NHSBSP).<sup>1-4</sup> The testing methods and standards applied are those of the relevant NHSBSP protocols, which are published as NHSBSP Equipment Reports. Report 14075 describes the testing of digital breast tomosynthesis systems.

The NHSBSP protocol is similar to the EUREF protocol,<sup>6</sup> but the latter also provides additional or more detailed tests and standards, some of which are included in this evaluation.

## 1.2 Objectives

The aim of the evaluation was to measure the technical performance of the GE Senographe Pristina system in tomosynthesis mode.

## 2. Methods

### 2.1 System tested

The tests were conducted at the GE factory in Buc, France, on the Pristina system. Details of the system tested are given in Table 1.

**Table 1. System description**

Manufacturer	GE Healthcare
Model	Senographe Pristina
System serial number	000011171069167144
Target material	Molybdenum (Mo), Rhodium (Rh)
Added filtration	30 $\mu$ m Mo, 30 $\mu$ m Silver (Ag)
Detector type	Caesium iodide (CsI) with amorphous silicon photodiode array
Detector serial number	VXA0005_07
Image pixel size	100 $\mu$ m
Detector size	240mm x 286mm
Pixel array	2394 x 2850
Source to table distance	637mm
Source to detector distance	660mm
Automatic exposure control (AEC) mode	AOP
Tomosynthesis projections	9 equal dose projections, equally spaced, covering range $\pm 12.5^\circ$
Centre of rotation	43mm above detector
Anti-scatter grid	Used in tomosynthesis exposures
Reconstructed focal planes	Focal planes at 0.5mm (default and used in this report) or 1mm intervals,
Slabs	10mm thickness with 5mm overlap between adjacent slabs.
Software version	1.13

The system can only select 1 of 3 different sets of radiographic factors using AEC. For 'radiological thicknesses' less than 35mm, 26kV Mo/Mo is used. For radiological thickness equal to or greater than 35mm, 34kV Rh/Ag is used. Radiological thickness is defined as the equivalent thickness of PMMA. The other set of radiographic factors 29kV, Mo/Mo, is used for magnification views and is not used in tomosynthesis mode.

In both 2D and tomosynthesis modes, Automatic Optimization of Parameters (AOP) is used for automatic exposure control (AEC). The system acquires a low dose image with a pre-pulse exposure. The signal in a small region of interest is examined to determine the appropriate radiographic factors. If the radiological thickness is predicted to exceed 80mm thickness of PMMA for tomosynthesis then an error message will be displayed, and it will not expose further. The radiographic factors selected for the pre-pulse are shown in Table 2.

**Table 2. Radiographic factors for pre-pulse exposures, selected according to compressed breast thickness (CBT)**

CBT	Radiographic factors
<38mm	26kV Mo/Mo, 2mAs
≥38mm and ≤65mm	34kV W/Ag, 2mAs
>65mm	34kV W/Ag, 4mAs

As the maximum compressed breast thickness (CBT) that can be reconstructed in tomosynthesis mode is 130mm, the system will prevent exposures for breasts exceeding that thickness.

The system has a static mode for tomosynthesis, in which the 9 projection images are acquired with the tube at 0°. This mode was used for measuring half value layer (HVL) and tube output.

The X-ray tube can travel from left to right or right to left depending on which one is the closer when starting the tomosynthesis exposure.

This system uses a moving anti-scatter grid that has been specifically designed for tomosynthesis. The grid lines are parallel to the tube motion.

There is no mode to automatically perform combination exposures, comprising a 2D and a tomosynthesis exposure in the same compression.

**Table 3. Image file sizes for 60mm CBT, 24cm x 29cm field size**

Format	Pixels per frame	Frames per image	Total image file size (MB)
Projections	2394x2850	9	120
Planes	2394x2850	145	1900
Slabs	2394x2850	17	200

Examples of the image file sizes are shown in Table 3. The file size of the reconstructed volume depends on the CBT and field size.

The Senographe Pristina is shown in Figure 1.



**Figure 1. The GE Senographe Pristina digital breast tomosynthesis system (image courtesy of GE Healthcare)**

## 2.2 Dose and contrast-to-noise ratio using AEC

### 2.2.1 Dose measurement

To calculate the MGD to the standard breast, measurements were made of HVL and tube output, at the 2 available kV and target/filter combinations. The output measurements were made on the midline at the standard position of 40mm from the chest wall edge (CWE) of the breast support platform. The compression paddle was in the beam, raised well above the ion chamber.

In tomosynthesis mode, exposures of a range of thicknesses of polymethyl methacrylate (PMMA) were made using AEC. For each measurement the height of the paddle was set to the equivalent breast thickness for that thickness of PMMA. Spacers were positioned at the nipple edge of the field, so as not to affect the operation of the AEC.

The method of measuring tomosynthesis doses described in the UK protocol differs slightly from the method described by Dance et al.<sup>7</sup> The incident air kerma is measured with the compression paddle well above, instead of in contact with, the ion chamber. Measurements on other systems<sup>1,2</sup> show that this variation reduces the air kerma and thus the mean glandular



dose (MGD) measurement by 3% to 5%. Otherwise the MGDs in tomosynthesis mode were calculated using the method described by Dance et al.<sup>7</sup>

This is an extension of the established 2D method, using the equation:

$$D = Kgc sT \quad (1)$$

where  $D$  is the MGD (mGy),  $K$  is the incident air kerma (mGy) at the top surface of the PMMA blocks, and  $g$ ,  $c$  and  $s$  are conversion factors. The additional factor,  $T$ , is derived by summing weighted correction factors for each of the tomosynthesis projections. Values of  $T$  are tabulated<sup>6</sup> for the GE Senographe Essential for different CBTs, and the same values are appropriate for the Pristina, because it has the same geometry.

### 2.2.2 Contrast-to-noise ratio

For contrast-to-noise ratio (CNR) measurements, a 10mm x 10mm square of 0.2mm thick aluminium foil was included in the PMMA phantom, positioned 10mm above the table on the midline, 60mm from the CWE.

The CNR was measured in the focal plane in which the aluminium square was brought into focus. The 5mm x 5mm regions of interests (ROI) were subdivided into 1mm x 1mm elements and the background ROIs were positioned adjacent to the aluminium square, as shown in Figure 2. The mean pixel values and their standard deviations were averaged over all the 1mm x 1mm elements, and the CNR was calculated from these averages.

CNR was also assessed in the unprocessed tomosynthesis projections acquired for these images and in the slabs.

The variation in central projection CNR with breast thickness and the variation in projection CNR with projection angle for a 53mm breast were also assessed.

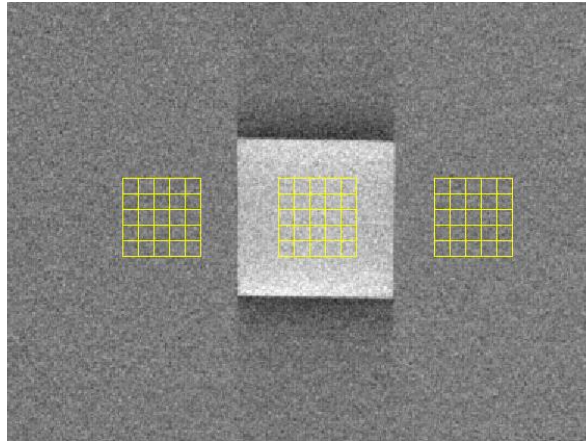


**Figure 2. The position of 5mm x 5mm ROIs for assessment of CNR (The CWE is to the left)**

### 2.3 Image quality measurements

A CDMAM phantom (Version 3.4, serial number 1022, UMC St. Radboud, Nijmegen University, Netherlands) was positioned between 2 blocks of PMMA, each 20mm thick. The exposure factors were chosen to be close to those selected by the AEC, when imaging a 50mm thickness of PMMA. This procedure was repeated to obtain a representative sample of 16 images at this dose level. Two further sets of 8 images at double and half this dose were then acquired.

The focal plane corresponding to the vertical position of the CDMAM phantom within the image was extracted from each reconstructed stack of images. The sets of CDMAM images were read and analysed using 2 software tools: CDCOM version 1.6 ([www.euref.org](http://www.euref.org)) and CDMAM Analysis version 2.1 (NCCPM, Guildford, UK). This was repeated for 2 focal planes immediately above and below the expected plane of best focus to ensure that the threshold gold thickness quoted corresponded to the best image quality obtained.

This analysis was repeated for the slab which included the height of the CDMAM phantom above the breast support table.

### 2.4 Geometric distortion and reconstruction artefacts

The relationship between reconstructed tomosynthesis focal planes and the physical geometry of the volume that they represent was assessed. This was done by imaging a geometric test phantom consisting of a rectangular array of 1mm diameter aluminium balls at 50mm intervals in the middle of a 5mm thick sheet of PMMA. The phantom was placed at various heights (7.5, 32.5, and 52.5mm) above the breast support table, within a 60mm stack of plain sheets of PMMA. Reconstructed tomosynthesis planes were analysed to find the height of the focal plane in which each ball was best in focus, the position of the centre of the ball within that plane, and the number of adjacent planes in which the ball was also seen. The variation in appearance of the ball between focal planes was quantified.

This analysis was automated using a software tool developed at the National Coordinating Centre for the Physics of Mammography (NCCPM) for this purpose. This software is in the form of a plug-in for use in conjunction with **ImageJ**.

### 2.4.1 Height of best focus

For each ball, the height of the focal plane in which it was best in focus was identified. Results were compared for all balls within each image, to judge whether there was any tilt of the test phantom relative to the reconstructed planes, or any vertical distortion of the focal planes within the image.

### 2.4.2 Positional accuracy within focal plane

The x and y co-ordinates within the image were found for each ball (x and y are perpendicular and parallel to the CWE, respectively). The mean distances between adjacent balls were calculated, using the pixel spacing quoted in the DICOM image header. This was compared to the physical separation of balls within the phantom, to assess the scaling accuracy in the x and y directions. The maximum deviations from the mean x and y separations were calculated, to indicate whether there was any discernible distortion of the image within the focal plane.

### 2.4.3 Appearance of the ball in adjacent focal planes

Changes to the appearance of a ball between focal planes were assessed visually.

To quantify the extent of reconstruction artefacts in focal planes adjacent to those containing the image of the balls, the reconstructed image was treated as though it were a true 3-dimensional volume. The software tool was used to find the z-dimension of a cuboid around each ball which would enclose all pixels with values exceeding 50% of the maximum pixel value. The method used was to re-slice the image vertically and create a composite x-z image using the maximum pixel values from all re-sliced x-z focal planes. A composite z line was then created using the maximum pixel from each column of the x-z composite plane, and a full width at half maximum (FWHM) measurement in the z-direction was made by fitting a polynomial spline. All pixel values were background subtracted using the mean pixel value from around the ball in the plane of best focus. The composite z-FWHM thus calculated (which depends on the size of the imaged ball) was used as a measure of the inter-plane resolution, or z-resolution.

## 2.5 Alignment

The alignment of the imaged volume to the compressed volume was assessed at the top and bottom of the volume. In order to assess vertical alignment, small high contrast markers (staples) were placed on the breast support table and on the underside of the compression paddle, and the image planes were inspected to check whether all markers were brought into focus within the reconstructed tomosynthesis volume. This was first done with no compression

applied and then repeated with the chest wall edge of the paddle supported and 100N compression applied.

## 2.6 Image uniformity and repeatability

The reproducibility of the tomosynthesis exposures was tested by acquiring a series of 5 images of a 45mm thick block of PMMA using AEC. A 10mm x 10mm ROI was positioned 60mm from the chest wall edge in the plane corresponding to a height of 22.5mm above the breast support table. The mean and standard deviation of the pixel values in the ROI were found and the SNR was calculated for each image. These images and others acquired during the course of the evaluation were evaluated for artefacts by visual inspection.

The set of 16 tomosynthesis CDMAM images was also used to test the repeatability of the reconstructed tomosynthesis images. The signal to noise ratio (SNR) was calculated just outside the CDMAM grid in the same position in the in-focus plane from each reconstructed image.

## 2.7 Detector response

The detector response was measured for the detector operating in tomosynthesis mode. A 2mm thick aluminium filter was placed in the beam and attached to the tube port. The compression paddle was removed. The 2 available beam qualities (26kV Mo/Mo, 34kV Rh/Ag) were selected and images were acquired using a range of tube load settings in tomosynthesis mode. The air kerma was measured and corrected using the inverse square law to give the air kerma incident at the detector. No corrections were made for the attenuation of X-rays by the breast support or anti-scatter grid. A 10mm x 10mm ROI was positioned on the midline, 50mm from the chest wall edge of the central projection image. The mean pixel value was measured and plotted against air kerma incident at the detector.

## 2.8 Timings

Using a stopwatch, image timings were measured while imaging a 45mm thickness of PMMA using AEC. Scan times were measured, from when the exposure button was pressed until the compression paddle was released, and to the moment when it was possible to start the next exposure. Reconstructed images were not displayed on the acquisition workstation, so the reconstruction time was not noted.

## 2.9 Modulation transfer function

Modulation transfer function (MTF) measurements were made in tomosynthesis projection images as described in the EUREF protocol,<sup>6</sup> at heights of 0mm and 40mm above the breast support table. Since the doses are low in the tomosynthesis projections and the MTF results are noisy, a 10th order polynomial fit was applied to the results.

## 2.10 Local dense area

This test is described in the EUREF protocol.<sup>6</sup> Images of a 30mm thick block of PMMA, of size 180mm x 240mm, were acquired using AEC. Extra pieces of PMMA between 2 and 20mm thick and of size 20mm x 40mm were added to provide extra attenuation. The compression plate remained in position at a height of 40mm, as shown in Figure 3. The simulated dense area was positioned 50mm from the CWE of the table.

In the simulated local dense area the mean pixel value and standard deviation for a 10mm x 10mm ROI were measured and the signal-to-noise ratios (SNRs) were calculated for the projection images.

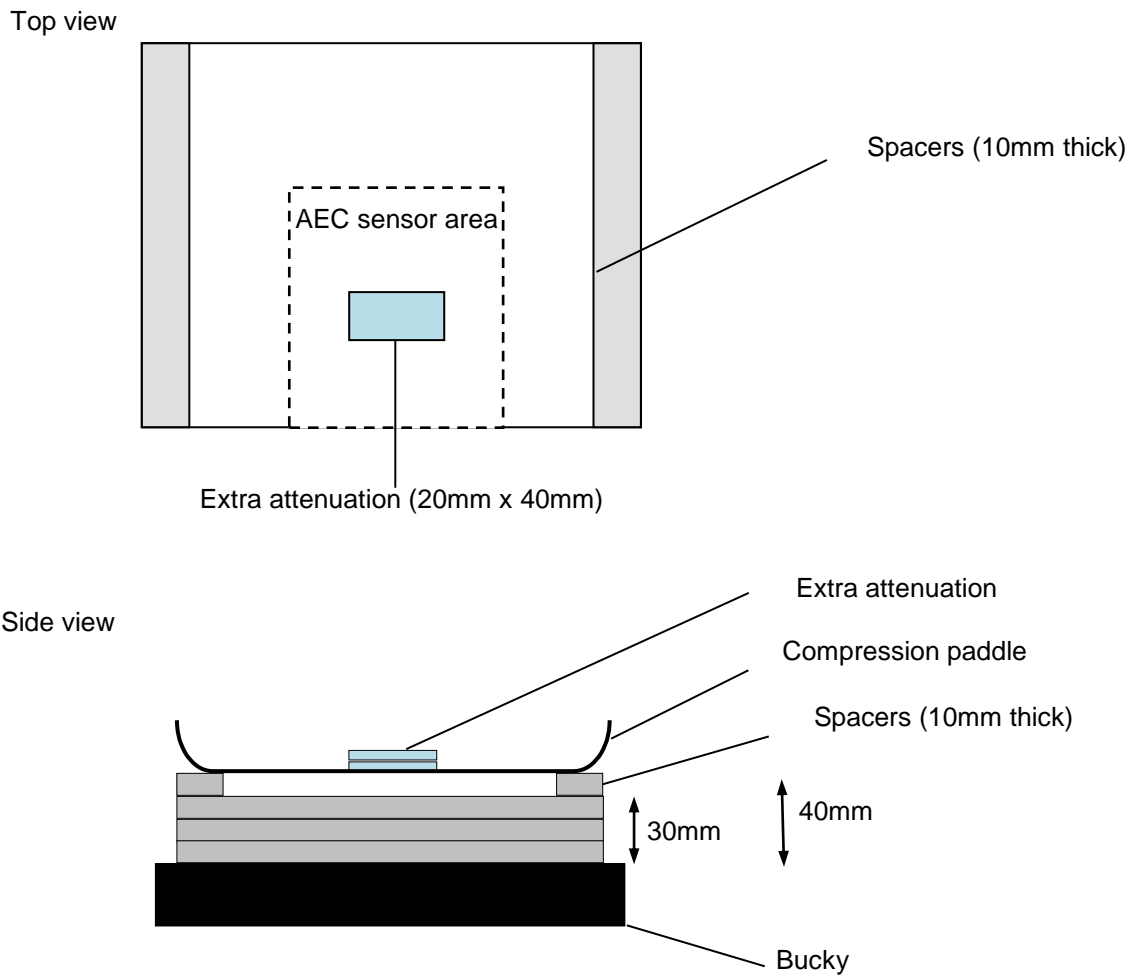


**Figure 3. Set-up to measure AEC performance for local dense areas**

### 3. Results

#### 3.1 Dose and contrast-to-noise ratio using AEC

The measurements of HVL and tube output of the system in tomosynthesis mode are summarised in Table 4.

**Table 4. HVL and tube output measurement in tomosynthesis mode**

kV	Target/filter	HVL (mm Al)	Output ( $\mu\text{Gy/mAs}$ at 1m)
26	Mo/Mo	0.34	26.7
34	Rh/Ag	0.54	45.2

The MGDs to the standard breast model are shown in Figure 4. All MGDs include the preliminary exposure, which is not included in the image. The dose limiting value from the EUREF protocol<sup>6</sup> is shown. The MGDs are shown in Table 5.

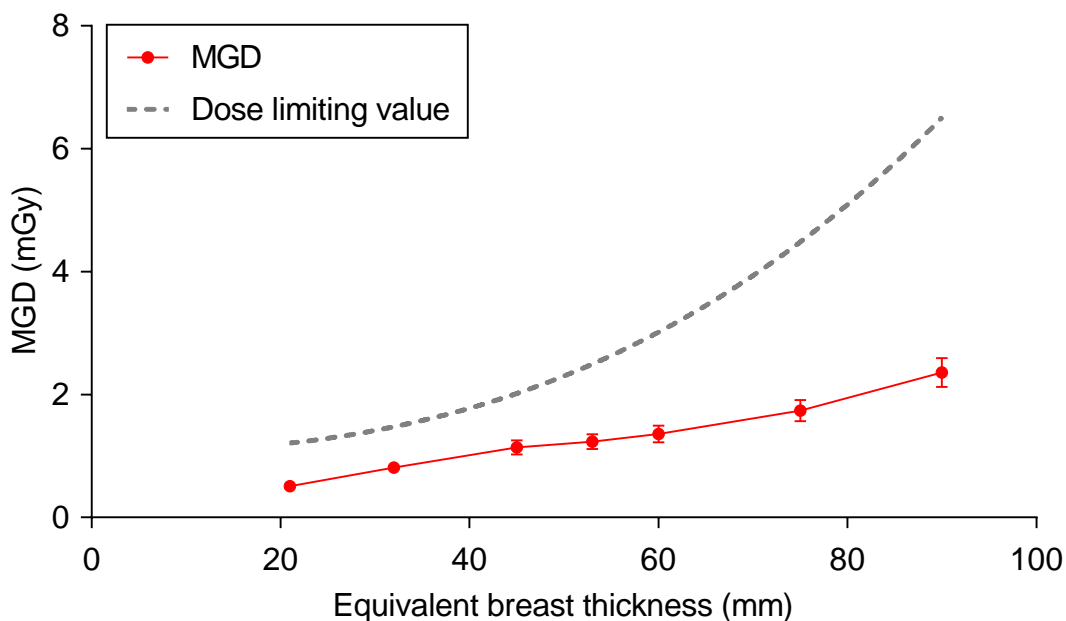


**Figure 4. MGD for tomosynthesis exposures acquired using AEC. Error bars indicate 95% confidence limits.**

**Table 5. Dose for tomosynthesis images acquired using AEC**

PMMA thickness (mm)	Equivalent breast thickness (mm)	kV	Target/filter	mAs	MGD (mGy)	Dose limiting value (mGy)	Displayed dose (mGy)	Displayed % higher than MGD
20	21	26	Mo/Mo	18.0	0.51	1.2	0.53	3.8%
30	32	26	Mo/Mo	39.6	0.81	1.5	0.84	4.3%
40	45	34	Rh/Ag	24.3	1.14	2.0	1.17	2.8%
45	53	34	Rh/Ag	28.9	1.23	2.5	1.28	4.2%
50	60	34	Rh/Ag	34.5	1.36	3.0	1.41	3.6%
60	75	34	Rh/Ag	49.0	1.74	4.5	1.84	5.7%
70	90	34	Rh/Ag	78.6	2.36	6.5	2.56	8.3%

Figure 5 shows the CNRs measured in focal planes, central projection images and slabs. The CNRs are shown in Table 6. Figure 6 shows the CNR in the projection images at different projection angles.

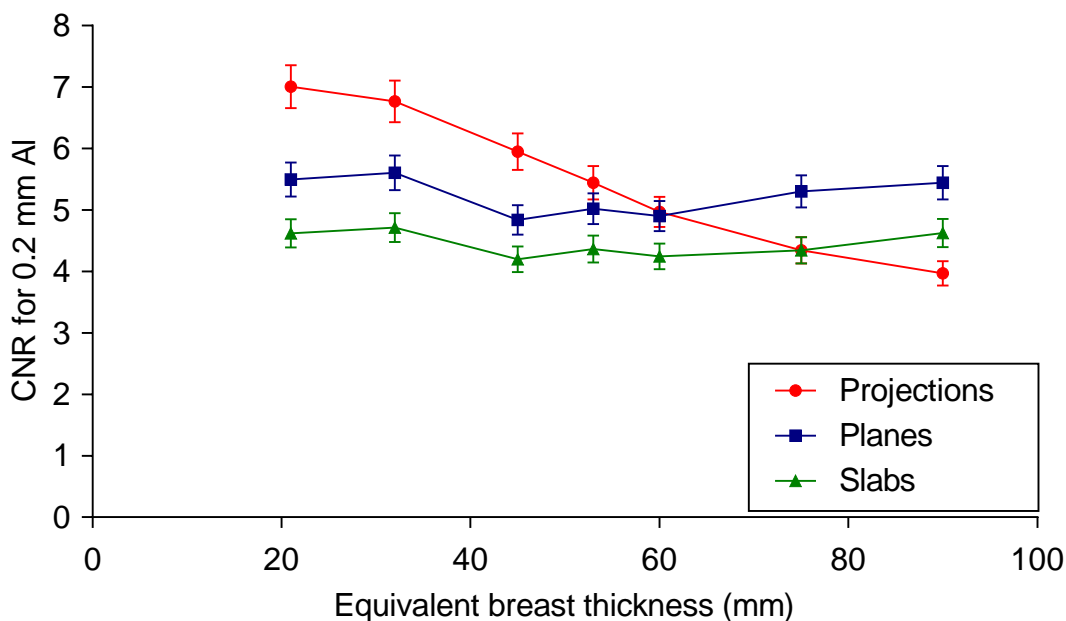


**Figure 5. CNR for tomosynthesis images acquired using AEC. Error bars indicate 95% confidence limits.**



**Table 6. CNR for tomosynthesis images acquired using AEC**

PMMA thickness (mm)	Equivalent breast thickness (mm)	kV	Target/ filter	mAs	CNR		
					Focal planes	Slabs	Central projections
20	21	26	Mo/Mo	18.0	5.49	4.62	7.00
30	32	26	Mo/Mo	39.6	5.60	4.72	6.77
40	45	34	Rh/Ag	24.3	4.84	4.20	5.95
45	53	34	Rh/Ag	28.9	5.02	4.36	5.45
50	60	34	Rh/Ag	34.5	4.90	4.24	4.97
60	75	34	Rh/Ag	49.0	5.31	4.35	4.35
70	90	34	Rh/Ag	78.6	5.44	4.62	3.97

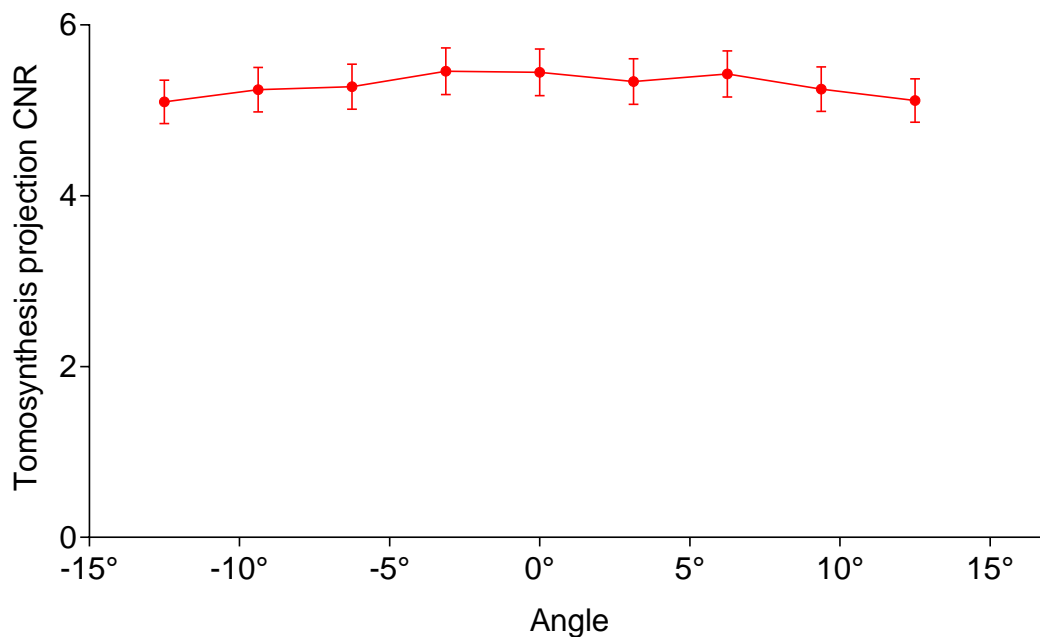


**Figure 6. Variation of projection CNR with angle for images of 45mm PMMA. Error bars indicate 95% confidence limits.**

### 3.2 Image quality measurements

The lowest threshold gold thicknesses were obtained for focal plane 54 and slab 5. In Figures 7 and 8, the threshold gold thicknesses are shown for focal plane 54 and slab 5 at approximately the AEC dose and twice and half the AEC dose. The threshold gold thicknesses shown in Figures 7 and 8 are summarised in Table 7.

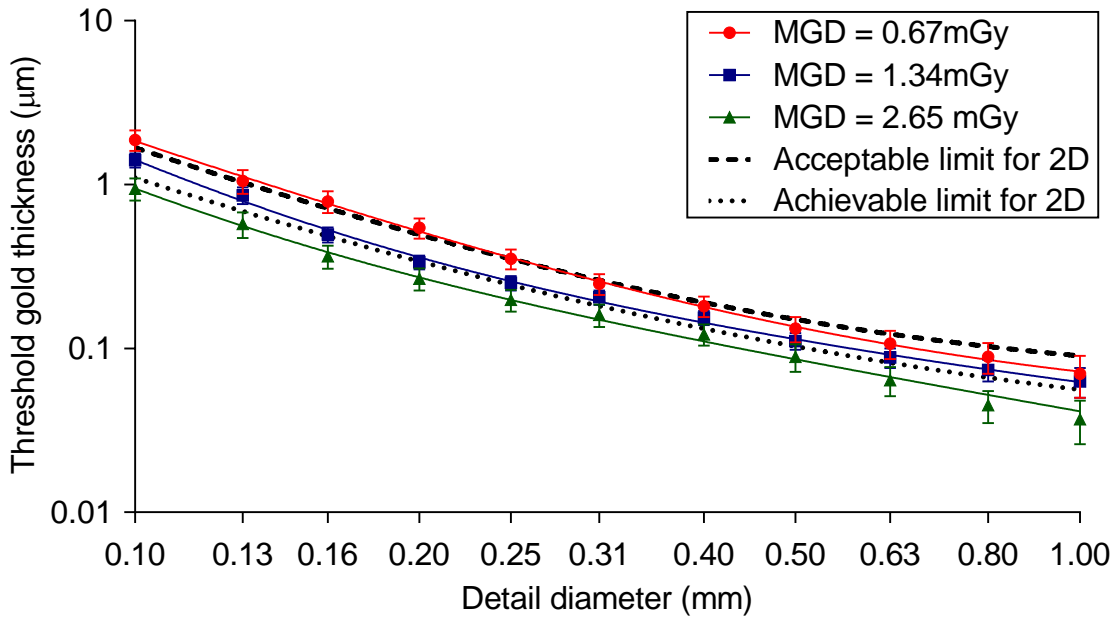


Figure 7. Threshold gold thickness for plane 54, at 3 dose levels. Error bars indicate 95% confidence limits.

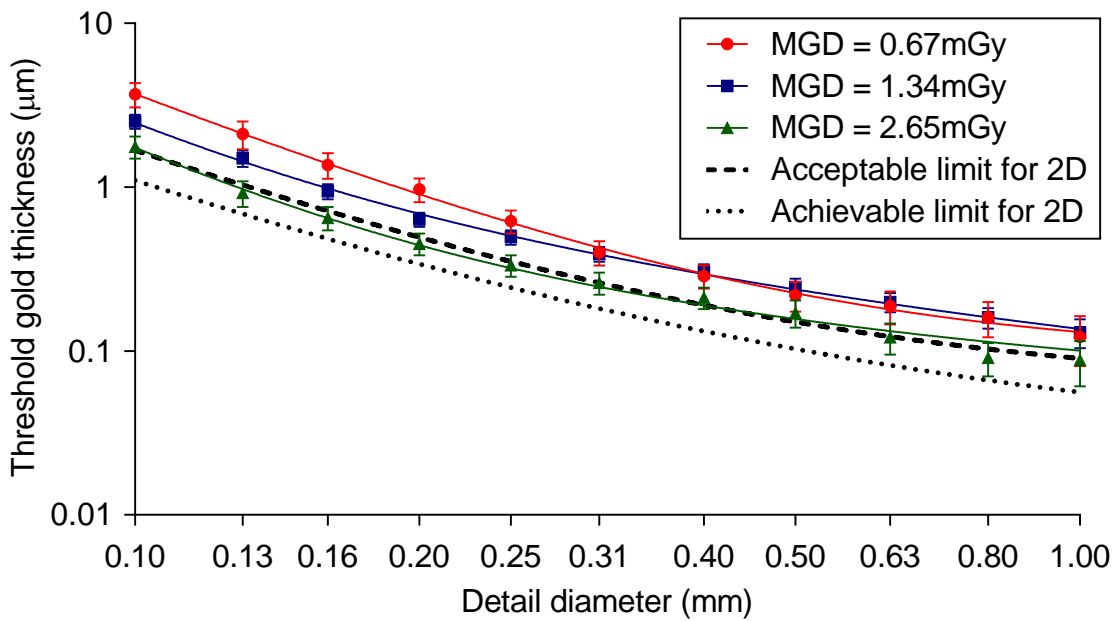


Figure 8. Threshold gold thickness for slab 5, at 3 dose levels. Error bars indicate 95% confidence limits.

**Table 7. Threshold gold thickness for reconstructed focal plane 54 and slab 5 of the image of the CDMAM phantom (automatically predicted data)**

Detail diameter (mm)	Threshold gold thickness ( $\mu\text{m}$ )					
	Plane (0.67mGy)	Plane (1.34mGy)	Plane (2.65mGy)	Slab (0.67mGy)	Slab (1.34mGy)	Slab (2.65mGy)
0.1	$1.87 \pm 0.27$	$1.41 \pm 0.14$	$0.95 \pm 0.15$	$3.69 \pm 0.62$	$2.20 \pm 0.22$	$1.77 \pm 0.27$
0.25	$0.35 \pm 0.05$	$0.25 \pm 0.03$	$0.20 \pm 0.03$	$0.62 \pm 0.10$	$0.40 \pm 0.04$	$0.33 \pm 0.05$
0.5	$0.13 \pm 0.02$	$0.11 \pm 0.01$	$0.089 \pm 0.017$	$0.22 \pm 0.05$	$0.17 \pm 0.02$	$0.17 \pm 0.03$
1.0	$0.070 \pm 0.020$	$0.063 \pm 0.013$	$0.037 \pm 0.011$	$0.12 \pm 0.04$	$0.096 \pm 0.019$	$0.088 \pm 0.027$

### 3.3 Geometric distortion and resolution between focal planes

#### 3.3.1 Height of best focus

All balls within each image (planes and slabs) were brought into focus at the same height ( $\pm 1\text{mm}$ ) above the table, and within 1mm of the expected height. This indicates that the focal planes are flat and parallel to the surface of the breast support table, with no noticeable vertical distortion.

Additional planes are reconstructed below the breast support table and above the compression paddle. The first focal plane corresponds to approximately 5mm below the breast support table. The last focal plane corresponds to approximately 7mm above the underside of the compression paddle. With the 0.5mm plane spacing used for testing, the number of focal planes reconstructed is equal to twice the indicated breast thickness in millimetre plus 25 for planes and 1/5 of the indicated breast thickness plus 2 for slabs.

#### 3.3.2 Positional accuracy within focal plane

No significant distortion or scaling error was seen within focal planes. Scaling errors, in both the x and y directions, were found to be less than 0.5%. Maximum deviation from the average distance between the balls was 0.18mm in the x and y directions, compared to the manufacturing tolerance of 0.1mm in the positioning of the balls.

#### 3.3.3 Appearance of the ball in adjacent focal planes

In the plane of best focus the aluminium balls appeared well defined and circular. When viewing successive planes, moving away from the plane of best focus, the images of the balls shrank in the direction parallel to the CWE. The changing appearance of one of the balls through successive focal planes and slabs is shown in Figures 9 and 10.

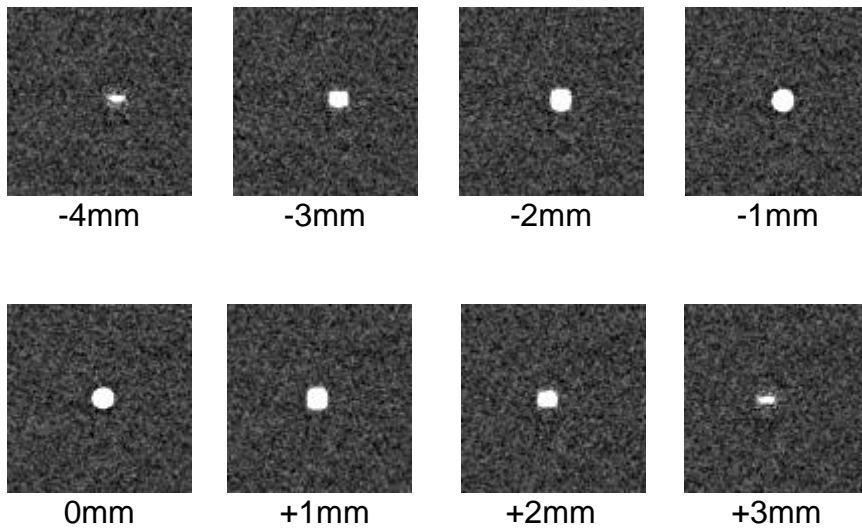


**Figure 9. Appearance of 1mm aluminium balls in reconstructed focal planes at 1mm intervals, from 4mm below to 3mm above the plane of best focus**

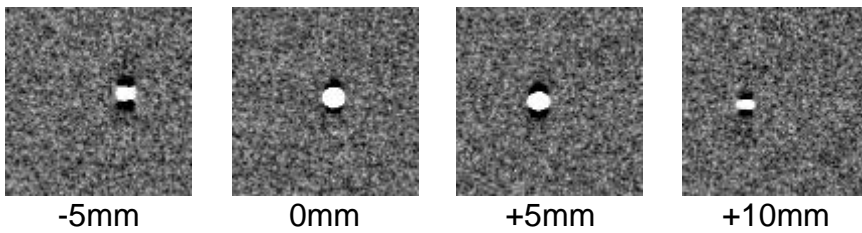


**Figure 10. Appearance of 1mm aluminium balls in reconstructed slabs at 5mm intervals, from 5mm below to 10mm above the slab of best focus**

Image extracts for a ball positioned in the central area, 120mm from the chest wall, are shown in Figure 11. In these images, pixels within the focal plane represent dimensions of approximately 0.1mm x 0.1mm. The spacing of reconstructed focal planes is 0.5mm.

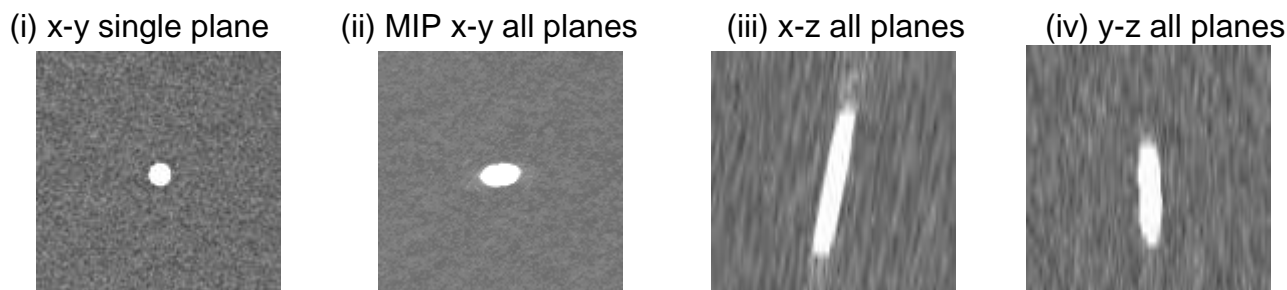


**Figure 11. Extracts from planes showing 1mm aluminium ball in (i) single focal plane, (ii) Maximum Image Projection (MIP) through all focal planes, and through re-sliced vertical planes in the directions (iii) parallel and (iv) perpendicular to the chest wall.**

Measurements of the z-FWHM of the reconstruction artefact associated with each ball are summarised in Table 8 for images of balls at heights of 7.5mm, 32.5mm and 52.5mm above the breast support table.

**Table 8. z-FWHM measurements of 1mm diameter aluminium balls**

	z-FWHM (range)
Planes	7.9mm (6.3 to 14.0)
Slabs	13.1mm (10.2 to 17.0)

### 3.4 Alignment

The staples on the breast support and under the paddle were brought into focus within the reconstructed volume. With 100N compression applied and only the chest wall edge of the paddle supported, the staples under the compression paddle near the CWE of the paddle were in focus within the reconstructed volume.

There was no missed tissue at the bottom or top of the reconstructed volume.

The chest wall edge of the breast support was measured to be 5mm from the edge of the detector. This was on the limit of acceptability.

### 3.5 Image uniformity and repeatability

In tomosynthesis mode the AEC selected the same tube voltage and target/filter combination for each of the 5 repeat exposures, and the tube load varied by a maximum of 1%. For exposures repeated during the 3 days of the evaluation the tube load varied by a maximum of 2%, within the 5% limiting value in the EUREF protocol.<sup>6</sup>

In the test of repeatability of the tomosynthesis reconstruction, using images of the CDMAM phantom, the maximum deviation from the mean SNR was found to be 2%.

The reconstructed images of plain PMMA were uniform with no visible artefacts.

### 3.6 Detector response

The detector response for the central projection of tomosynthesis images acquired at 26kV Mo/Mo and 34kV Rh/Ag, with anti-scatter grid, is shown in Figure 12.

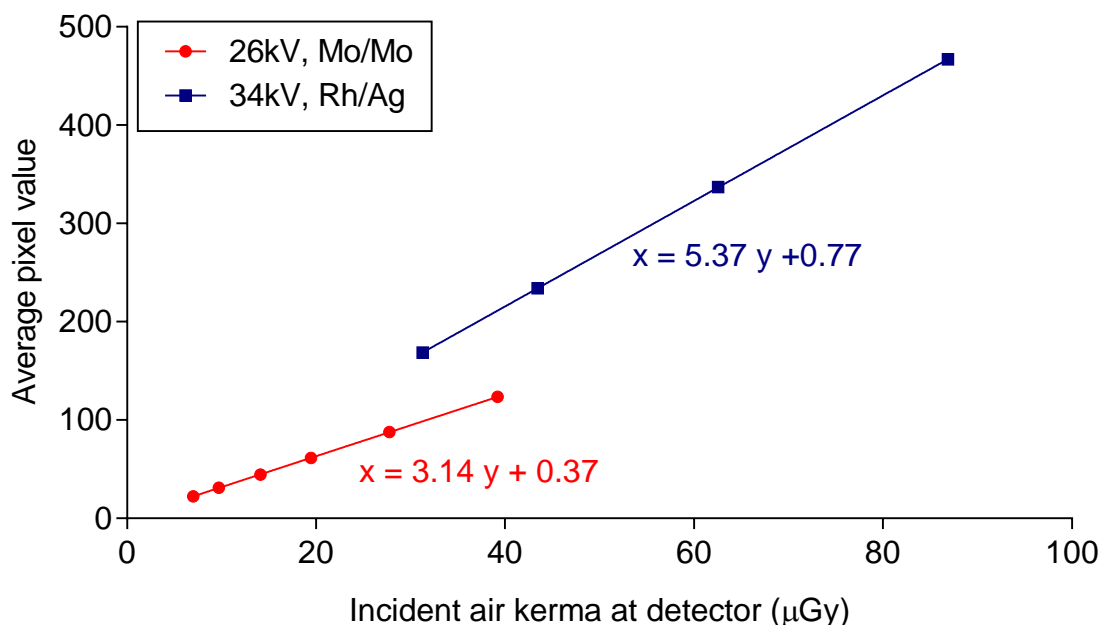


**Figure 12. Detector response in tomosynthesis mode**

### 3.7 Timings

Scan times are shown in Table 9. The tomosynthesis images are reconstructed within the acquisition workstation and then sent to a review workstation for display. A review station was not available and so the time from decompression until the reconstructed image is displayed was not measured.

**Table 9. Scan and reconstruction timings**

	Time
Time from start of exposure until decompression	9s
Time from start of exposure until next exposure is possible	17s
Time from decompression until reconstructed image displayed	not measured

### 3.8 Modulation transfer function

MTF results for the central projection images are shown in Figure 13. Results are shown in the 2 orthogonal directions parallel (u) and perpendicular (v) to the tube axis, at 0mm and 40mm above the surface of the breast support table. These results are summarised in Table 10.

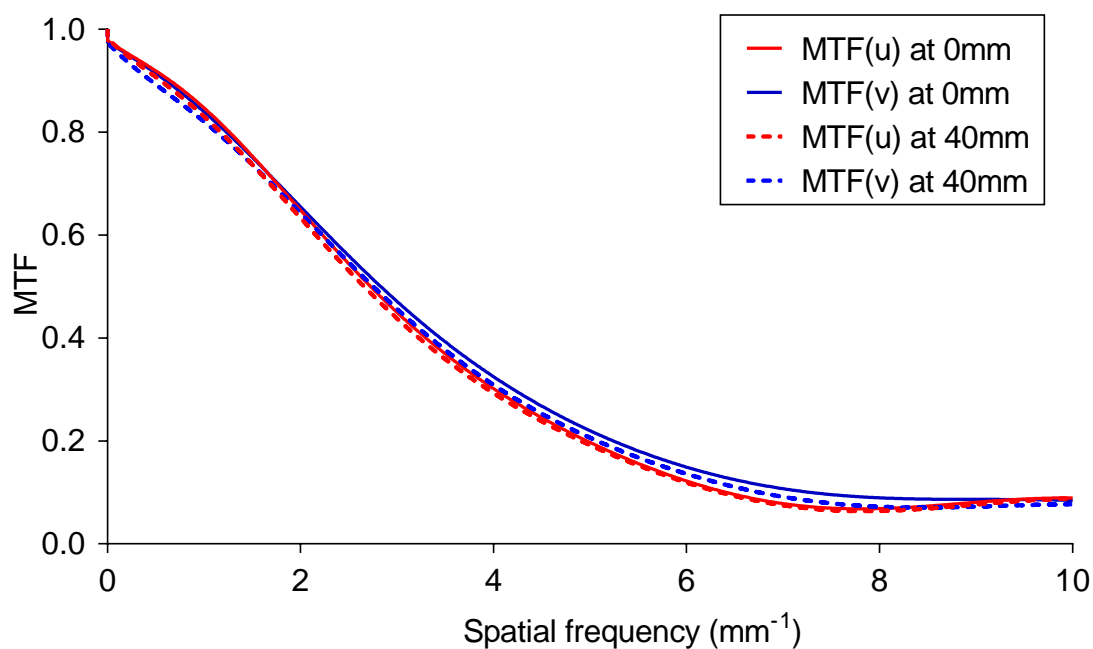


**Figure 13. MTF for central projections**

**Table 10 MTF for central projections in the directions parallel (u) and perpendicular (v) to the tube axis**

Spatial frequency (mm <sup>-1</sup> )	0mm above table		40mm above table	
	u	v	u	v
0	1.00	1.00	1.00	1.00
1	0.85	0.84	0.83	0.82
2	0.65	0.66	0.63	0.64
3	0.45	0.47	0.44	0.46
4	0.30	0.32	0.29	0.31
5	0.20	0.22	0.19	0.21
6	0.12	0.15	0.12	0.14
7	0.08	0.11	0.07	0.09
8	0.07	0.09	0.06	0.07
9	0.08	0.09	0.08	0.07
10	0.09	0.08	0.09	0.08

The spatial frequencies of the 50% MTF (MTF<sub>50</sub>) are shown in Table 11.

**Table 11 MTF<sub>50</sub> for central projection**

	u-direction	v-direction
0mm	2.73mm <sup>-1</sup>	2.83mm <sup>-1</sup>
40mm	2.66mm <sup>-1</sup>	2.75mm <sup>-1</sup>

### 3.9 Local dense area

Exposures were found to vary with addition of the small pieces of PMMA, indicating that the AEC adjusts for local dense areas in tomosynthesis mode. The system changed from 26kV Mo/Mo to 34kV Rh/Ag between 34mm and 36mm of total thickness of PMMA. It was expected to switch at 35mm.

The test in the EUREF protocol<sup>6</sup> is based on an assumption that when the AEC adjusts for local dense areas, the SNR should remain constant with increasing thickness of extra PMMA. The results are presented in Table 12 and Figure 14. The results show a large change in SNR between 34mm and 36mm of PMMA, accompanied by a change in the kV and anode/filter combination. This results in SNR differences from the mean SNR value of larger than the 20% tolerance.<sup>6</sup> If the SNR results for only the 34kV, Rh/Ag are used, then the SNR are within the 20% tolerance. It should be noted that this tolerance was set in the protocol for a base of 40mm PMMA rather than 30mm PMMA used in this report.

**Table 12. AEC performance for local dense areas, measured on the midline and 50mm from the CWE**

Total attenuation (mm PMMA)	kV	Target/ filter	Tube load (mAs)	SNR	% SNR difference from mean SNR result of	
					all SNRs	only 34kV, Rh/Ag
32	26	Mo/Mo	43.0	13.2	-24%	-
34	26	Mo/Mo	55.1	13.3	-23%	-
36	34	Rh/Ag	20.2	20.0	14%	7%
38	34	Rh/Ag	21.4	19.6	12%	5%
40	34	Rh/Ag	23.0	18.9	10%	3%
42	34	Rh/Ag	24.6	18.8	8%	1%
44	34	Rh/Ag	26.4	18.2	6%	-1%
46	34	Rh/Ag	27.8	18.2	2%	-4%
48	34	Rh/Ag	29.4	17.4	-5%	-11%



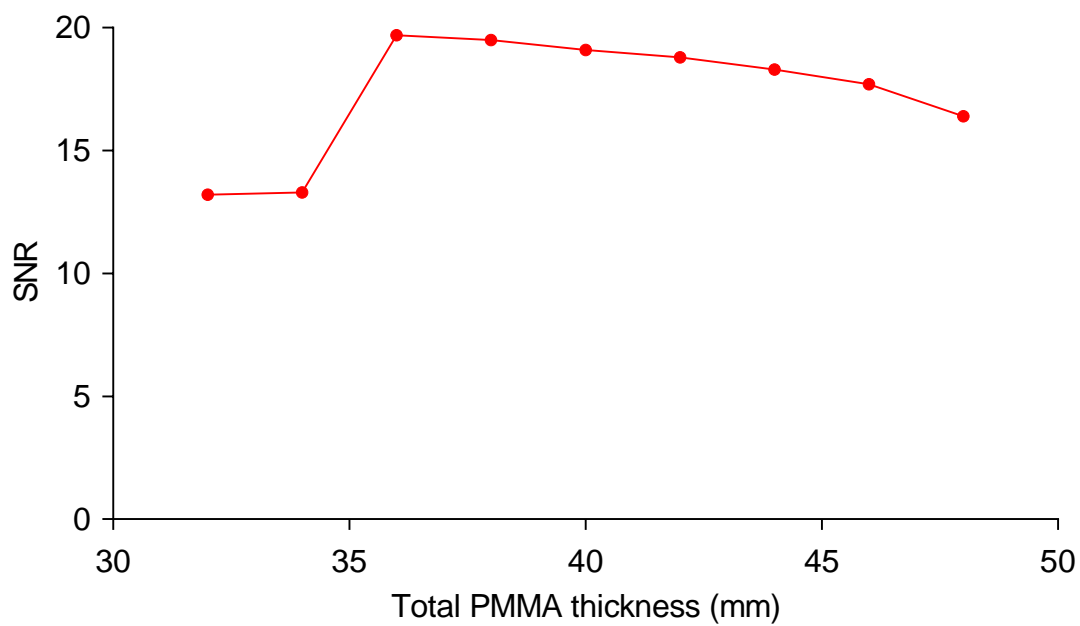


**Figure 14. AEC performance in projection images for local dense areas**

## 4. Discussion

### 4.1 Dose and contrast-to-noise ratio

The MGDs in tomosynthesis mode were lower than the dose limiting values set for tomosynthesis systems in the EUREF protocol.<sup>6</sup>

CNRs in projections showed a steady decrease with increasing breast thickness, but the CNRs in the resultant reconstructed planes and slabs were relatively constant with breast thickness.

### 4.2 Image quality

In the absence of any better test object for assessing tomosynthesis imaging performance, images of the CDMAM test object were acquired in tomosynthesis modes. At the dose close to that selected by the AEC, the threshold gold thickness for reconstructed focal planes was better than the minimum acceptable level and, for detail diameters greater than 0.13mm, close to the achievable level of image quality that is applied to 2D mammography. Results were determined for focal plane number 54 and slab 5, which gave the best results for planes and slabs respectively. For double and half the AEC selected dose, the threshold gold thickness changed as expected.

These results take no account of the ability of tomosynthesis to remove the obscuring effects of overlying tissue in a clinical image, and the degree of this effect is expected to vary between tomosynthesis systems. There is as yet no standard test object that would allow a realistic and quantitative comparison of tomosynthesis image quality between systems or between 2D and tomosynthesis modes. A suitable test object would need to incorporate simulated breast tissue to show the benefit of removing overlying breast structure in tomosynthesis imaging, as compared to 2D imaging.

### 4.3 Geometric distortion and reconstruction artefacts

Assessment of geometric distortion demonstrated that the reconstructed tomosynthesis focal planes were flat and parallel to the surface of the breast support table. No vertical or in-plane distortion was seen and there were no significant scaling errors.

The reconstructed tomosynthesis volume starts about 5mm below the surface of the breast support table and continues 8mm above the nominal height of the compression paddle. This is useful in that it allows for a small margin of error in the calibration of the indicated thickness or some slight tilt of the compression paddle, without missing tissue at the bottom or top of the reconstructed image.

The mean inter-plane resolution (z-FWHM) for the 1mm diameter balls was 7.9mm and 13.1mm for the planes and slabs respectively.

#### 4.4 Alignment

The alignment of the X-ray beam to the reconstructed image was satisfactory.

There was no missed tissue at the bottom or top of reconstructed tomosynthesis images.

The distance between the chest wall edge and the detector was 5mm. This is on the limit in the EUREF protocol.<sup>6</sup>

#### 4.5 Image uniformity and repeatability

The repeatability of tomosynthesis AEC exposures and the repeatability of tomosynthesis reconstructions were satisfactory with values of between 1 and 2%, well below the limit of 5%.

#### 4.6 Modulation transfer function

There are only small differences in the MTFs between the 2 orthogonal directions and there is little reduction in the MTF at 40mm above the breast support. The system uses step and shoot acquisition and so the x-ray tube is stationary during exposure. There is some geometric blurring due to the size of the focal spot. The effect on the MTF is small at this height, according to Marshall and Bosmans, 2012.<sup>8</sup> The effect of step and shoot and tube motion during acquisition on the MTF of the projection tomosynthesis images is explored in a paper by Mackenzie et al.<sup>9</sup>

#### 4.7 Local dense area

The EUREF protocol<sup>6</sup> states that the system is expected to adjust the exposures in response to the thickness of added PMMA. A provisional tolerance was that the SNR is kept within 20% of the average SNR.

The GE Senographe Pristina undertakes a low dose pre-exposure to set the radiographic factors. The factors are adjusted according to the densest area detected in the image. However, there is a large change in SNR when the exposure factors change with added thickness of PMMA. If a 40mm thick block of PMMA had been used for this test (as described in the EUREF protocol<sup>6</sup>), then the change in kV and anode/filter combination would have been avoided. The appropriateness of the 20% tolerance is in doubt if a system changes the radiographic factors as the PMMA is added, as occurred here. For this system, using only the SNR results for radiographic factors of 34kV, Rh/Ag, then the results were within the 20% tolerance.

## 5. Conclusions

The technical performance of the GE Senographe Pristina digital breast tomosynthesis system was found to be satisfactory, although image quality standards have not yet been established for digital breast tomosynthesis systems.

The MGD to the 53mm thick standard breast in tomosynthesis mode was found to be 1.23mGy. This is below the dose limiting value of 2.5mGy for tomosynthesis.<sup>6</sup>

## References

1. Studley CJ, Looney P, Young KC. Technical evaluation of Hologic Selenia Dimensions digital breast tomosynthesis system (NHSBSP Equipment Report 1307 Version 2). Sheffield: NHS Cancer Screening Programmes, 2014
2. Strudley CJ, Warren LM, Young KC. Technical evaluation of Siemens Mammomat Inspiration digital breast tomosynthesis system (NHSBSP Equipment Report 1306 Version 2). Sheffield: NHS Cancer Screening Programmes, 2015
3. Strudley CJ, Oduko JM, Young KC. Technical evaluation of GE Healthcare SenoClaire digital breast tomosynthesis system (NHSBSP Equipment Report 1404). London: Public Health England, 2016
4. Strudley CJ, Hadjipanteli A, Oduko JM, Young KC. Technical evaluation of Fujifilm AMULET Innovality digital breast tomosynthesis system (NHSBSP Equipment Report). London: Public Health England, 2018
5. Burch A, Loader R, Rowberry B et al. Routine quality control tests for breast tomosynthesis (physicists) (NHSBSP Equipment Report 1407). London: Public Health England, 2015
6. van Engen RE, Bosmans H, Bouwman RW et al. Protocol for the Quality Control of the Physical and Technical Aspects of Digital Breast Tomosynthesis Systems. Version 1.03. [www.euref.org](http://www.euref.org) 2018
7. Dance DR, Young KC, van Engen RE. Estimation of mean glandular dose for breast tomosynthesis: factors for use with the UK, European and IAEA breast dosimetry protocols. *Phys. Med. Biol.*, 2011, 56, 453-471.
8. Marshall N W and Bosmans H. Measurements of system sharpness for two digital breast tomosynthesis systems. *Phys. Med. Biol.*, 2012, 57, 7629–50
9. Mackenzie A, Marshall NW, Hadjipanteli A et al. Characterisation of noise and sharpness of images from four digital breast tomosynthesis systems for simulation of images for virtual clinical trials. *Phys. Med. Biol.*, 2017, 62, 2376-2397